Origin of magnetic stochasticity and transport in plasma microturbulence

D.R. Hatch,[1] M. J. Pueschel,[1] F. Jenko,[1] W. M. Nevins,[2] P. W. Terry,[3] and H. Doerk[1]

[1]*Max-Planck-Institut für Plasmaphysik, EURATOM Association, 85748 Garching, Germany*
[2]*Lawrence Livermore National Laboratory, Livermore, California 94550, USA*
[3]*University of Wisconsin-Madison, Madison, Wisconsin 53706, USA*

Nonlinear excitation of linearly stable microtearing modes – with zonal modes acting as a catalyst – is shown to be responsible for the near-ubiquitous magnetic stochasticity and associated electromagnetic electron heat transport in gyrokinetic simulations of plasma microturbulence.

Introduction.– To date, many key aspects of turbulent transport in magnetized fusion plasmas remain poorly understood. This includes, in particular, the origin and role of magnetic field fluctuations which are observed in both experiments and simulations. These fluctuations evolve self-consistently with other turbulent quantities and allow heat to be transported radially via electrons streaming along perturbed field lines. The relative importance of this effect is expected to increase with the normalized plasma pressure, β. Since high β is desirable for many aspects of high-performance discharges (reaction rates, e.g., scale like β^2), unravelling the characteristics of turbulent transport in this regime is an active and important area of current research.

Over the last few years, gyrokinetic simulations have provided some surprising results concerning electromagnetic effects in plasma microturbulence (see, e.g., Refs. [1–6]). Notably, in the case of ion temperature gradient (ITG) turbulence, systematic β scans [4, 5] have been performed, showing that the electromagnetic electron heat transport increases roughly as β^2 until it becomes comparable to the electrostatic contributions. Moreover, the resulting magnetic field fluctuations exhibit fully developed stochasticity even at low values of β.[7–9] Both of these empirical findings are puzzling and cannot be understood on the basis of quasilinear theory. The latter predicts a linear transport scaling with β, as well as negligible stochasticity, given that ITG modes are not well-structured to break magnetic field lines.

Via novel analysis techniques (developed for the study of damped eigenmode excitation [10–12]) applied to electromagnetic gyrokinetic simulations with the GENE code [1], we provide an explanation for both observations which is outside the standard theoretical framework of plasma microturbulence. While traditionally, turbulent transport in the plasma core has been linked almost exclusively [13] to linearly unstable modes, the scenario that emerges here is that linearly damped, but nonlinearly driven microtearing modes become important or even dominant at high β. Moreover, it is shown that the relevant excitation mechanism involves a nonlinear coupling with zonal modes, defined here as fluctuations at $k_y = 0$. This definition encompasses both the zonal

flow and other fluctuations, such as the geodesic acoustic mode [14] (k_y is the Fourier wavenumber for the mostly-poloidal binormal direction). Zonal modes are well known to play a critical role in moderating turbulent saturation levels. In contrast, here we introduce another role of zonal modes as the catalyst of an additional transport mechanism.

Simulation setup.– Much of the data used in the following analysis is taken from the GENE dataset described in Ref. [5]. The widely used Cyclone Base Case [15] parameters are employed, with the addition of finite electron plasma beta $\beta = 8\pi n_e T_{e0}/B_0^2$ (where n_e and T_{e0} are the background electron density and temperature, and B_0 is the magnitude of the background magnetic field), ranging from the electrostatic limit to $\beta = 0.012$. The reader is referred to Ref. [5] for a detailed description of the physical and numerical parameters.

Occurrence of tearing structures.– In a first step, we demonstrate the presence of tearing structures in the turbulence, and show that they are responsible for the observed magnetic stochasticity and transport. Tearing structures are perturbations which have a resonant component of the parallel magnetic vector potential, $A_{||}$. The resonant component can be extracted by integrating along the field line at a q-rational surface, where q is the safety factor. A structure with tearing parity – even symmetry for $A_{||}$ along the field line – will typically have a strong resonant component. In contrast, a structure with ballooning parity – odd parity along the magnetic field, as is characteristic of the ITG mode – will have no resonant component. In order to identify tearing structures, we construct proper orthogonal decompositions (POD) [16, 17] of $A_{||}$. This yields $A_{||}(z,t) = \sum_n A_{||}^{(n)}(z) h^{(n)}(t)$, where z is the coordinate parallel to the magnetic field, and both the mode structures, $A_{||}^{(n)}(z)$, and the time traces, $h^{(n)}(t)$, are orthogonal and arranged in order of decreasing amplitude.

More specifically, we seek to decompose $A_{||}$ into components with even and odd parity, corresponding, respectively, to subdominant tearing modes and ITG modes, as it will turn out. We do this by constructing a POD of every linearly independent set of wavenumbers in the full $A_{||k_x,k_y}(z,t)$ dataset, where k_x is the radial Fourier
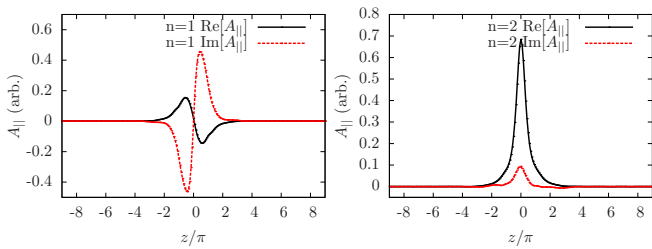
FIG. 1: Typical $A_{||}$ POD modes structures. The $n = 1$ mode (left) has ballooning parity and the $n = 2$ mode (right) has tearing parity.

wavenumber. A linearly independent set of wavenumbers consists of a single k_y wavenumber, and all k_x wavenumbers that define its extended mode structure, i.e., the k_x modes which are connected by the flux tube parallel boundary condition [18] and are identical to the k_x modes that are resolved in a corresponding linear simulation. It is observed that the $n = 1$ POD mode structure matches very closely the mode structure of the unstable ITG mode at wavenumbers with strong linear drive. This is an indication of the effectiveness of this analysis in separating the role of the most unstable ITG modes from that of subdominant modes. The first two $A_{||}$ POD modes almost invariably define a clear ballooning component and a clear tearing component. An example is shown in Fig. 1, where the $n = 1$ and $n = 2$ modes are plotted for $\beta = 0.003$, and $k_y \rho_s = 0.2, k_x \rho_s = 0$ (where $\rho_s = (m_i T_{e0})^{1/2} / e B_0$ is the sound radius). As will be shown, almost all of the stochasticity and transport can be captured with only these two modes (i.e., the first two POD modes for each wavenumber).

When the central k_x value is non-zero, the modes may peak away from the outboard midplane ($z = 0$) and also exhibit some mixing of the parity. Even in these cases, there typically remains one mode which is predominantly tearing and one which is predominantly ballooning. In order to automatically distinguish the ballooning components from the tearing components, a parity factor is defined, $P = |\int dz A_{||}| / \int dz |A_{||}|$. The parity factor is zero for pure ballooning parity and may approach a value of one for tearing parity modes. This can be used to decompose the entire $A_{||}$ dataset according to

$$A_{||_{k_x,k_y}}(z,t) = A_{||}^{(ball)} + A_{||}^{(tear)} + A_{||}^{(res)}, \qquad (1)$$

where the ballooning component ($ball$) is defined as whichever of the first two POD modes has the smaller parity factor, the tearing component ($tear$) is whichever of the first two POD modes has the larger parity factor, and the rest of the POD modes are grouped into the residual category (res).

This analysis procedure can be summarized as follows: (1) Select from the $A_{||}$ fluctuation data a single k_x and k_y, along with all k_x modes connected by the parallel boundary condition. (2) Construct a POD of this data set. (3) Select from the first two POD modes the one with the largest parity factor and group it in the tearing component of the decomposition. (4) Select from the first two POD modes the one with the smaller parity factor and group it in the ballooning component of the decomposition. (5) Repeat steps 1-4 for all sets of wavenumbers in the dataset. The result is a decomposition [as defined in Eq. (1)] of $A_{||_{k_x,k_y}}(z,t)$ which defines a dominant ballooning component and a dominant tearing component.

Stochasticity and transport due to tearing structures.– With this tearing-ballooning decomposition in hand, we can study the contribution of each component to the magnetic field fluctuations and transport. In order to do this, a routine is used to follow the trajectory of magnetic field lines and track their deviation from the equilibrium field. Poincaré plots verify that the tearing component produces a fully stochastic field, i.e., the field lines are no longer confined to flux surfaces, but rather fill the simulation volume. This can be quantified with a magnetic diffusivity $D_{fl} = \lim_{l \to \infty} \langle [r_i(l) - r_i(0)]^2 \rangle / l$, [8] where r_i is the radial position of the ith field line, l is the distance traced along the field line, and an average is taken over all traced field lines. Across the β scan, the tearing component of $A_{||}$ produces a magnetic diffusivity that is comparable to that of the total $A_{||}$, while the ballooning and residual components produce comparatively negligible diffusivities.

In Refs. [8, 9], the magnetic diffusivity is shown to have quite a direct relation to the electron electromagnetic heat transport, $Q_e^{EM} = \langle \tilde{q}_{e||} \tilde{B}_x \rangle / B_0$, where $\langle \rangle$ denotes a spatial average, $\tilde{q}_{e||}$ is the parallel heat flux moment, and $\tilde{B}_x$ is the radial component of the fluctuating magnetic field. Using the tearing-ballooning decomposition, we can directly calculate different contributions to Q_e^{EM}. The Q_e^{EM} k_y spectra are quite distinctive (see, e.g., Fig. 6b in Ref. [4]); they exhibit a dip in the flux at the same scales where the electrostatic transport channel peaks. This dip dominates at low β and becomes less prominent as β increases. The present analysis shows that this feature is the result of the superposition of the transport associated with the ITG modes and the stochastic transport associated with the subdominant tearing modes, as will be described below.

Using the decomposition defined in Eq. (1), one can define a ballooning component of the flux, $\langle \tilde{q}_{e||} \tilde{B}_x^{ball} \rangle / B_0$, a tearing component, $\langle \tilde{q}_{e||} \tilde{B}_x^{tear} \rangle / B_0$, and the residual, $\langle \tilde{q}_{e||} \tilde{B}_x^{res} \rangle / B_0$. The k_y flux spectra (at $\beta = 0.003$) for the different components are shown in Fig. 2. The ballooning component of the flux defines a heat pinch that peaks in the low k_y region where the ITG modes dominate. In contrast, the tearing component of the transport is outward, also peaking at low k_y, but additionally extending with significant amplitude to the higher wavenumbers in the spectrum. The total transport spectrum is a super-
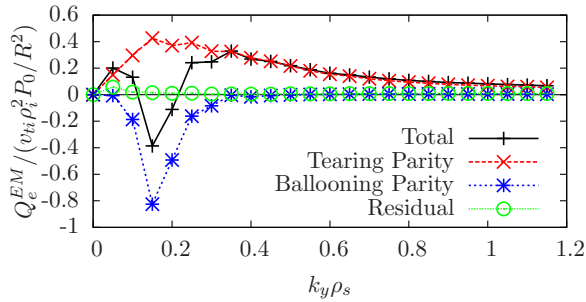
FIG. 2: The total electromagnetic electron heat flux spectrum (plus signs), summed over k_x for $\beta = 0.003$, decomposed into contributions from tearing modes (crosses), balloon modes (asterisks) and all remaining fluctuations (circles).
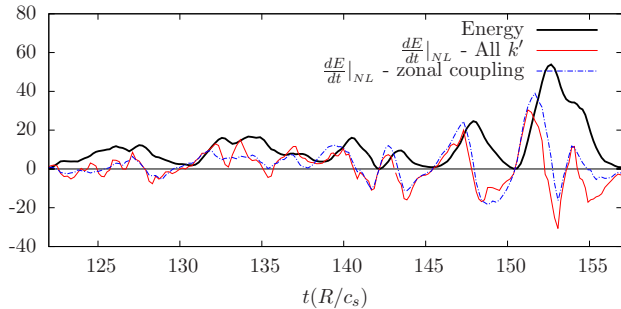

FIG. 3: The free energy in the POD tearing mode (solid black line) at $k_x\rho_s = 0$, $k_y\rho_s = 0.2$, and $\beta = 0.003$ along with the total nonlinear drive (gray line–red online) and the nonlinear drive defined by coupling with zonal wavenumbers (dashed line–blue online), plotted over a time segment of the nonlinear saturated state. The energetics of the tearing mode is dominated by the nonlinear drive which consists largely of the zonal coupling.

position of these two contributions. In order to further elucidate the components of the transport, we express the parallel heat flux in terms of the parallel temperature gradient along a perturbed field line,[2]

$$\tilde{q}_{e\|} = -n_{0e}\chi_{e\|}\left(\frac{d\tilde{T}_{e\|}}{dz} + \frac{\tilde{B}_x}{B_0}\frac{d\tilde{T}_{e\|}}{dx} + \frac{\tilde{B}_x}{B_0}\frac{dT_{e0}}{dx}\right), \quad (2)$$

where n_{0e} is the electron density and $\chi_{e\|}$ is the parallel electron heat conductivity. As it turns out, the ITG modes mainly contribute via the first term which scales like β,[5] while the third term is closely related to the field line diffusivity, D_{fl}, and describes the heat transport due to streaming along stochastic field lines. The latter is produced by the tearing structures; it scales like β^2 and thus dominates as β increases.

Nonlinear excitation via zonal modes.– Having demonstrated the role of tearing structures in the magnetic stochasticity and transport, we turn now to identifying an excitation mechanism. To this end, we first construct

a POD of the gyrocenter distribution function from a GENE simulation and examine the energetics of the tearing fluctuations. We examine in detail the wavenumber $k_y\rho_s = 0.2$, $k_x\rho_s = 0$ for the $\beta = 0.003$ case. The $n = 4$ mode in the POD exhibits clear tearing parity and also defines the dominant outward contribution to the electromagnetic heat flux. In order to examine the excitation mechanism of this mode, we construct nonlinear energy transfer functions.[19] The free energy is defined as $E_{\mathbf{k}} = \sum_j \int dz dv_{\|} d\mu T_{j0}/F_{j0} \left(g_{j\mathbf{k}} + q_j F_{j0}/T_{j0}\chi_{j\mathbf{k}}\right)^* g_{j\mathbf{k}}$, where $v_{\|}$ and μ are the two velocity coordinates, j denotes the particle species, g_j is the gyrocenter distribution function, q_j is particle charge, F_{j0} is the background Maxwellian distribution function, $\chi_j = \bar{\phi}_j + v_{Tj}v_{\|}\bar{A}_{\|j}$, where the overbar denotes a gyroaverage, and v_{Tj} is the particle thermal velocity. The corresponding energy evolution equation is

$$\partial_t E_{\mathbf{k}} = \mathcal{L}[g_{\mathbf{k}}, g_{\mathbf{k}}] + \sum_{k_x',k_y'}\mathcal{N}[g_{\mathbf{k}}, g_{\mathbf{k}'}, g_{\mathbf{k}-\mathbf{k}'}] + c.c., \quad (3)$$

where $\mathcal{L}$ includes the linear gyrokinetic operator, and the nonlinear energy transfer function $\mathcal{N}$ is defined as

$$\mathcal{N}_{\mathbf{k},\mathbf{k}'} = \sum_j \int dz dv_{\|} d\mu \left(k_x' k_y - k_x k_y'\right)$$
$$[q_j\chi_{j\mathbf{k}}^*\chi_{j\mathbf{k}'}g_{j(\mathbf{k}-\mathbf{k}')} - T_{j0}/F_{j0}g_{j\mathbf{k}}^*\chi_{j(\mathbf{k}-\mathbf{k}')}g_{j\mathbf{k}'}]. \quad (4)$$

The latter represents the energy transferred conservatively between the wavenumbers (k_x, k_y) and (k_x', k_y') as evidenced by the property, $\mathcal{N}_{\mathbf{k},\mathbf{k}'} = -\mathcal{N}_{\mathbf{k}',\mathbf{k}}$. This, however, defines the nonlinear energy transfer function for all fluctuations at a given wavenumber; a refinement is necessary to examine the energetics of the tearing mode of interest: $\partial_t E_{\mathbf{k}}^{(tear)} = \mathcal{L}[g_{\mathbf{k}}^{(tear)}, g_{\mathbf{k}}] + \sum_{\mathbf{k}'}\mathcal{N}[g_{\mathbf{k}}^{(tear)}, g_{\mathbf{k}'}, g_{\mathbf{k}-\mathbf{k}'}]$, where $g^{(tear)}$ represents the POD tearing mode described above, and the LHS represents the evolution of the tearing mode energy because of the orthogonality of the POD modes. It is observed that the nonlinear energy transfer for the tearing mode is dominated by energy injected *into* the mode from wavenumbers at the same k_y and $|k_x| > 0$, and energy transferred *out* of the mode into zonal wavenumbers ($k_y = 0$). Note that both of these energy transfer channels represent coupling with zonal modes. A closer examination shows that the energetics of the mode is dominated by the imbalance between this energy transfer as demonstrated in Fig. 3 where the free energy of the tearing mode is plotted along with the total nonlinear drive and the component of the nonlinear drive defined by the subset of wavenumbers representing zonal coupling: $k_y'\rho_s = 0.2$ and $k_y'\rho_s = 0$. This subset captures the major trends in the energy balance. The linear term in the energy equation (not shown in Fig. 3) occasionally plays a role but is, in general, much smaller than the nonlinear term which dominates both the drive and saturation of the tearing mode. We thus
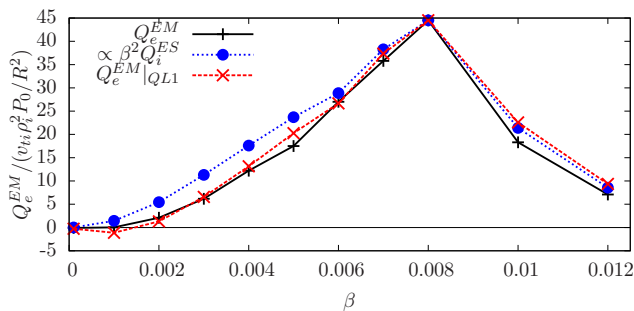
FIG. 4: Q_e^{EM} plotted over the β scan (plus signs) along with a model estimating the flux as a fixed fraction of $\beta^2 Q_i^{ES}$ (circles), and a model with an additional correction (crosses) defined by the quasilinear magnetic flux associated with the most unstable mode.

have the unique situation where the saturation mechanism for the driving ITG instability in turn produces a significant additional transport channel.

Tearing structures are microtearing modes.– One may now ask if this POD tearing mode finds an analog in the linear eigenmode spectrum. An examination of the linear spectrum reveals several marginally stable tearing parity modes which are essentially electrostatic in nature. In order to find a mode which produces the transport described above, we employ a direct eigenvalue solver (incorporated into the GENE code, see Ref. [20]) that resolves all eigenmodes in the spectrum, but is very numerically demanding. A reduced resolution test case [$(9, 16, 32, 8)$ grid points in $(k_x, z, v_{||}, \mu)$] reveals one eigenmode which has a tearing mode structure largely matching the POD mode described above and also produces a significant value of Q_e^{EM}. A series of numerical tests indicate that this mode is a legitimate microtearing mode similar to those described in Ref. [21]: The mode is sensitive to changes in the electron temperature gradient but not the ion temperature gradient, it is fundamentally changed in the electrostatic limit but not when the electrostatic potential is artificially deleted. For this problem, linear convergence tests are, ironically, more demanding than nonlinear convergence tests. Careful nonlinear convergence tests were performed and reported in Ref. [5]. These tests have been augmented by a high k_x resolution GENE simulation ($k_{x_{max}}\rho_s = 11.9$) which shows no significant change in the transport quantities.

A simple transport model.– The scenario described above implies that a significant component of the transport is not directly attributable to the driving instabilities. Such a situation is clearly not captured by quasilinear theory. Here we describe a first attempt to devise a simple model that reproduces the observed β dependence of Q_e^{EM}, using as inputs the ion electrostatic heat flux and one free parameter that can be determined at a single point in the scan.

The nonlinear nature of the tearing mode excitation motivates the hypothesis that the level of electromagnetic electron heat flux (due to the tearing modes) can be modelled as a fixed fraction of the ion electrostatic heat transport (due to the dominant instabilities) multiplied by the appropriate factor of β^2: $Q_e^{EM}(\beta) = C_0\beta^2 Q_i^{ES}$. In Fig. 4, this estimate is plotted across the β scan along with the total value of Q_e^{EM} (C_0 is calculated at $\beta = 0.008$). This model can be improved by also accounting for the contribution of the ITG modes themselves to Q_e^{EM}. This is done with the quasilinear estimate $Q_e^{EM(ball)} = Q_i^{ES}(Q_e^{EM}/Q_i^{ES})_{MU}$, where $(Q_e^{EM}/Q_i^{ES})_{MU}$ is the ratio of fluxes for the most unstable linear eigenmode (ITG mode at lower β and trapped electron mode at higher β) at the peak of the spectrum ($k_y\rho_s = 0.15$). This estimate, $Q_e^{EM} = Q_i^{ES}\left\{C_0\beta^2 + (Q_e^{EM}/Q_i^{ES})_{MU}\right\}$, is also plotted in Fig. 4. Its merit is reflected in the improved agreement at lower β where the inward ballooning transport is a non-negligible fraction of the whole.

Summary.– In this Letter, we have shown that magnetic stochasticity and transport in ITG turbulence is caused by linearly stable microtearing modes that are excited by nonlinear coupling to zonal wavenumbers. These insights are expected to improve the understanding and control of magnetized high β plasmas.

[1] F. Jenko *et al.*, Phys. Plasmas **7**, 1904 (2000).
[2] F. Jenko and W. Dorland, Plasma Phys. Controlled Fusion **43**, A141 (2001).
[3] S. E. Parker *et al.*, Phys. Plasmas **11**, 2594 (2004).
[4] J. Candy, Phys. Plasmas **12**, 072307 (2005).
[5] M. J. Pueschel, M. Kammerer, F. Jenko, Phys. Plasmas **15**, 102310 (2008).
[6] M. J. Pueschel and F. Jenko, Phys. Plasmas **17**, 062307 (2010).
[7] M.J. Pueschel, Ph.D. Thesis, Universität Münster (2009).
[8] W. M. Nevins *et al.*, Phys. Rev. Lett. **106**, 065003 (2011).
[9] E. Wang *et al.*, Phys. Plasmas **18**, 056111 (2011).
[10] P. W. Terry *et al.*, Phys. Plasmas **13**, 022307 (2006).
[11] D. R. Hatch *et al.*, Phys. Rev. Lett. **106**, 115003 (2011).
[12] D. R. Hatch *et al.*, Phys. Plasmas **18**, 055706 (2011).
[13] For an exception see, e.g., B. D. Scott, Phys. Rev. Lett. **65**, 3289 (1990).
[14] P.H. Diamond *et al.*, Plasma Phys. Controlled Fusion **47**, R35 (2005).
[15] A. M. Dimits *et al.*, Phys. Plasmas **7**, 969 (2000).
[16] G. Berkooz, P. Holmes, and J. L. Lumley, Annu. Rev. Fluid Mech. **25**, 539 (1993).
[17] S. Futatani *et al.*, Phys. Plasmas **16**, 042506 (2009).
[18] M. A. Beer *et al.*, Phys. Plasmas **2**, 2687 (1995).

[19] C. Holland *et al.*, Nucl. Fusion **43**, 761 (2003).

[20] M. Kammerer *et al.*, Phys. Plasmas **15**, 052102 (2008).

[21] H. Doerk *et al.*, Phys. Rev. Lett. **106**, 155003 (2011).